

Separation of Linear and Star Chains by a Nanopore

Hui Ge[†] and Chi Wu^{*†,‡}

[†]Department of Chemistry, The Chinese University of Hong Kong, Shatin, N.T., Hong Kong, and [‡]The Hefei National Laboratory of Physical Science at Microscale, Department of Chemical Physics, The University of Science and Technology of China, Hefei, Anhui 230026, China

Received August 12, 2010

Revised Manuscript Received September 29, 2010

The separation of polymer chains with different topologies but a similar hydrodynamic volume still remains as a real, important, and challenging problem in polymer research because we often face a mixture of polymer chains with different topologies due to the nature of some preparation methods. For example, there are usually two ways to prepare star chains with different arms, namely, the core first or the arm first.¹ In the core-first method, a multifunctional initiator is used to initiate polymerization of monomers. Such obtained star chains often have different arm numbers and lengths because not all of the initiating sites are simultaneously activated. In the arm-first method, linear polymer chains with a uniform length and an active end are first synthesized, often by anionic polymerization, and then they are coupled together with a multifunctional core. In order to make sure that each of the reactive sites on the core is attached with one arm, the number of linear chains must be much larger than that of active sites on the core. After such a coupling reaction, one inevitably has a mixture of linear and star chains. For star chains with few arms, their hydrodynamic volume is not much different from that of individual arms so that a conventional size exclusion chromatography (SEC) is not able to effectively and cleanly separate them. Previously, Meunier and co-workers^{2–4} tried to use different flow rates to separate polymer chains with different topologies by extruding a mixture of them through some monolithic columns packed with specially prepared polystyrene latex particles, which involves some unclear size exclusion mechanisms.

Recently, we experimentally confirmed a previous prediction; namely, there exist a critical flow rate ($q_{c,linear}$) for linear polymer chains to pass through a nanopore under an elongational flow field,^{5,6} and such a critical flow rate is independent of the chain length but related to the pore diameter (D) as⁷ $q_{c,linear} = (k_B T / 3\pi\eta) k^{-1} D^{1-(1/\nu)}$, where k_B , T , and η are the Boltzmann constant, the absolute temperature, and the solvent viscosity, respectively; k is a constant for a given polymer solution, but $1/2 \leq \nu \leq 3/5$, depending on the solvent quality.⁸ The measured $q_{c,linear}$ leads to a corresponding hydrodynamic force that is needed to overcome the entropic force of a coiled chain. Note that this force is much weaker than the previously measured enthalpic ones in the 1990s.⁹ It is energetically favored for star chains with f arms to crawl through a nanopore under an elongational flow by a symmetrical mode, i.e., putting a half number of their arms forward. In such a mode,^{10,11} there also exists a critical flow rate $q_{c,star} = q_{c,linear}(f/2)$. Note that linear chains are a special kind of star chain with $f = 2$. It is clear from a theoretical point of view that even for $f = 3$, $q_{c,star}$ is still 1.5 times higher than $q_{c,linear}$.

*To whom correspondence should be addressed at the Hong Kong address.

Therefore, it is practically possible to separate linear and star chains by flushing a mixture of them through a nanopore with a properly chosen flow rate.

To test such a possibility, we synthesized polystyrene (PS) linear and star chains (up to 41 arms) with different lengths by using divinylbenzene to couple living polystyrene linear chains in solution. The details can be found elsewhere.^{1,12,13} We further fractionate such prepared star chains into a series of narrowly distribution star chains with different numbers of arms.¹⁴ The 3-arm star chains was previously synthesized by using chlorosilane as the coupling agent.¹² The molecular parameters, such as the weight-average molar mass (M_w), the polydispersity index (M_w/M_n), and average hydrodynamics radius ($\langle R_h \rangle$) characterized by laser light scattering (LLS), of such obtained star chains as well as three linear chains used are summarized in Table 1.

A modified commercial LLS spectrometer (ALV/DLS/SLS-5022F) equipped with a multi- τ digital time correlator (ALV5000) and a cylindrical 22 mW UNIPHASE He–Ne laser ($\lambda_0 = 632$ nm) was used to characterize each solution before and after it passes through the nanopores. The incident beam was vertically polarized with respect to the scattering plane. The details of the instrumentation and theory can be found elsewhere.¹⁵ In static LLS, the excess absolute time-averaged scattered light intensity, known as the excess Rayleigh ratio $R_{vs}(\theta)$, of a very dilute polymer solution at an infinite small angle is proportional to the weight-average molar mass (M_w). In dynamic LLS, the intensity–intensity time correlation function ($G^{(2)}(\tau)$) is measured. Each measured $G^{(2)}(\tau)$ is related to a normalized field–field autocorrelation function $|g^{(1)}(\tau)|$. The Laplace inversion of $g^{(1)}(\tau)$ leads to a line-width distribution $G(\Gamma)$ that can be converted to a hydrodynamic radius distribution $f(R_h)$ by the Stokes–Einstein equation.^{15–17} Note that the inversion is an ill-conditioned problem. The positions of the peaks in $G(\Gamma)$ or $f(R_h)$ might slightly vary with the fitting conditions but have less effect on the area ratio of the peaks. In this study, all the dynamic LLS results presented were obtained at the scattering angle of 20°.

In our ultrafiltration experiments, a double-layer membrane filter (Whatman, Anotop 10) was used. The top and bottom layers contain an equal number of 200 and 20 nm cylindrical pores, respectively; i.e., each large pore is on top of a small pore. Such a structure prevents any possible interference of the flow fields generated by different small pores at their entrances. Note that we purposely added a certain amount of short reference PS chains with a size smaller than 20 nm in each solution. These short chains will pass the nanopore even without any flow so that they served as an internal reference. The concentrations of star, linear, and reference chains (C_S , C_L , and C_R) are properly chosen so that $\langle I_S \rangle / \langle I_R \rangle = C_S M_S / C_R M_R \sim 1$ and $\langle I_L \rangle / \langle I_R \rangle = C_L M_L / C_R M_R \sim 1$, where “ $\langle I_S \rangle$ ”, “ $\langle I_L \rangle$ ”, and “ $\langle I_R \rangle$ ” and “ M_S ”, “ M_L ”, and “ M_R ” are the average scattered light intensity and the molar masses of star, linear, and reference chains, respectively. In dynamic LLS, $\langle I_S \rangle / \langle I_R \rangle$ and $\langle I_L \rangle / \langle I_R \rangle$ are proportional to the area ratio of their corresponding peaks in $G(\Gamma)$. The scattered light intensity is proportional to the square of mass of a scattering subject. Therefore, the decrease of $\langle I_S \rangle / \langle I_R \rangle$ or $\langle I_L \rangle / \langle I_R \rangle$ sensitively reflects the retention of star or linear chains by the nanopore.¹⁸ The solution temperature (T) and the flow rate (q) were precisely controlled by an incubator (Stuart Scientific, S160D) (± 0.1 °C) and a syringe pump (Harvard Apparatus, PHD 2000), respectively.

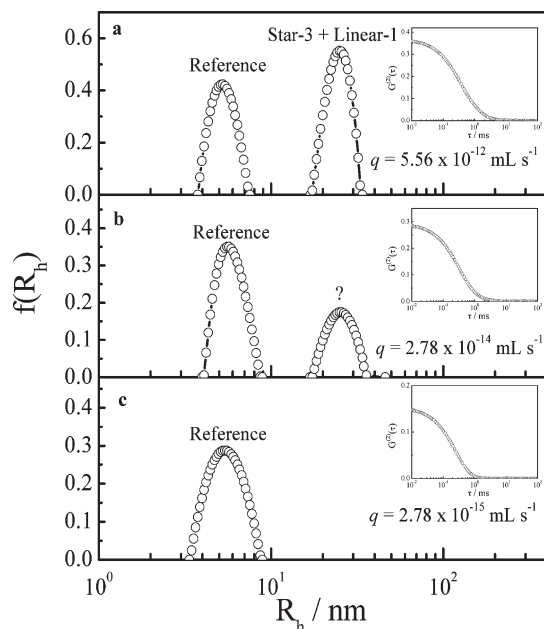


Figure 1. Hydrodynamic radius distribution of a mixture of reference, linear-1, and star-3 chains in toluene at $T = 25\text{ }^{\circ}\text{C}$ after the solution is extruded through nanopores under different elongational flow rates, where $C_{\text{reference}} = 1.20 \times 10^{-2}\text{ g/mL}$, $C_{\text{linear-1}} = 2.50 \times 10^{-4}\text{ g/mL}$, and $C_{\text{star-3}} = 3.80 \times 10^{-4}\text{ g/mL}$. Insets are corresponding time autocorrelation functions.

Table 1. Summary of Star, Linear, and Reference Polymer Chains Used in This Study

polymers	f	$M_{w,\text{arm}}/(\text{g mol}^{-1})$	$M_{w,\text{star}}/(\text{g mol}^{-1})$	M_w/M_n	$\langle R_h \rangle/\text{nm}$
reference	2	2.15×10^4	4.30×10^4	1.04	5
linear-1	2	2.95×10^5	5.90×10^5	1.01	22
linear-2	2	9.00×10^6	1.80×10^7	1.08	160
star-3	3	2.10×10^5	6.30×10^5	1.08	32
star-41	41	2.10×10^5	8.61×10^6	1.20	61

Figure 1 shows how star-3 and linear-1 chains in a mixture are separated by different flow rates. When the flow rate is $5.56 \times 10^{-12}\text{ mL s}^{-1}$, higher than $q_{c,\text{star}}$ ($5.43 \times 10^{-14}\text{ mL s}^{-1}$ for star-3), we observed two peaks, as shown in Figure 1a, very similar to those before the extrusion, indicating that both star-3 and linear-1 chains have passed through the nanopore under such a flow. Note that star-3 and linear-1 chains have a similar average hydrodynamic size so that they appear as one peak in $f(R_h)$. As the flow rate decreases to $2.78 \times 10^{-14}\text{ mL s}^{-1}$, lower than $q_{c,\text{star}}$ (star-3) but higher than $q_{c,\text{linear}}$ ($1.94 \times 10^{-14}\text{ mL s}^{-1}$), Figure 1b shows that the peak located at $\sim 25\text{ nm}$ shrinks, revealing, in principle, that star-3 chains in the solution mixture are retained, but we are not really sure about it. This is why we put a question mark on it. Figure 1c shows that further decrease of the flow rate to $2.78 \times 10^{-15}\text{ mL s}^{-1}$, lower than $q_{c,\text{linear}}$, only one peak related to reference chains appears after the extrusion, clearly demonstrating that both star-3 and linear-1 chains are not able to pass through the nanopore under this condition.

In order to prove that at $q = 2.78 \times 10^{-14}\text{ mL s}^{-1}$, only linear chains have passed through the nanopore; we further mixed much bigger star-41 chains with linear-1 chains so that we can resolve them in $f(R_h)$. Figure 2a shows two well-separated peaks located at ~ 25 and $\sim 60\text{ nm}$, when the flow rate is much higher than both $q_{c,\text{star}}$ and $q_{c,\text{linear}}$, very similar to those before the extrusion. This is expected because both star-41 and linear-1 chains have passed through the nanopore under this condition. When the flow rate is decreased to the range $q_{c,\text{linear}} < q < q_{c,\text{star}}$ (star-41), Figure 2b

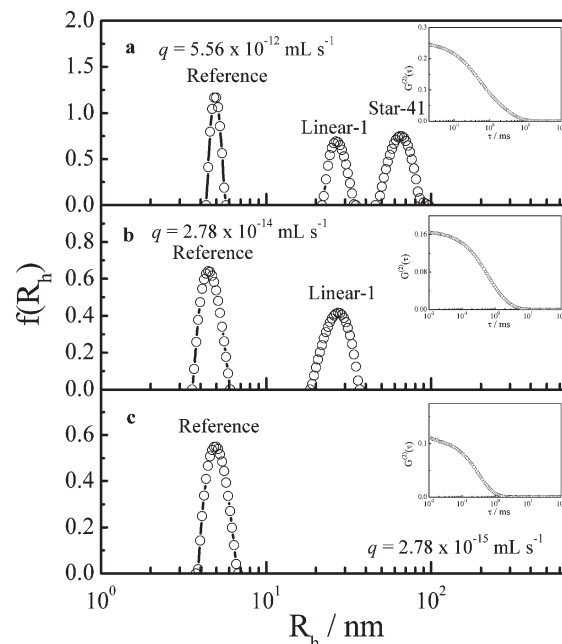


Figure 2. Hydrodynamic radius distribution of a mixture of reference, linear-1, and star-41 chains in toluene at $T = 25\text{ }^{\circ}\text{C}$ after the solution is extruded through nanopores under different elongational flow rates, where $C_{\text{reference}} = 2.00 \times 10^{-2}\text{ g/mL}$, $C_{\text{linear-1}} = 8.00 \times 10^{-4}\text{ g/mL}$, and $C_{\text{star-41}} = 1.00 \times 10^{-4}\text{ g/mL}$. Insets are corresponding time autocorrelation functions.

shows that the peak associated with star-41 completely disappears, presumably, retained by the filter. It clearly shows that we are able to effectively and cleanly separate star-41 and linear-1 chains by using a properly chosen flow rate. As expected, further decrease of the flow rate to $q < q_{c,\text{linear}}$, the peak associated with linear-1 chains also vanishes (Figure 2c). Therefore, we are not only able to separate star and linear chains by a properly chosen flow rate but also able to fractionate them by gradually increasing q .

An attentive reader might say, ‘‘Of course, this is just a size effect, not related to the chain topology, because star-41 chains are much bigger than linear-1 chains.’’ To prove that such a separation is indeed due to the topology, not the size, of polymer chains, we have further mixed smaller star-3 chains with relatively bigger linear-2 chains. As expected, both linear-2 and star-3 chains are able to pass through the nanopore when q is higher than both $q_{c,\text{star}}$ and $q_{c,\text{linear}}$, appearing as two distinguished additional peaks in Figure 3a. The decrease of the flow rate into the range $q_{c,\text{linear}} < q < q_{c,\text{star}}$ (star-3) results in the block of star-3 chains, as shown in Figure 3b, even though they are smaller than linear-2 chains, clearly demonstrating that the separation of polymer chains in our experiment is due to different chain topologies, not their sizes. As expected, Figure 3c shows that when the flow is sufficiently low, both star-3 and linear-2 chains are retained. It is worth noting that for the convenience of discussion we have shown the results in a decreasing order of the flow rate. In a real separation/fractionation experiment, we increase q step-by-step so that linear chains pass first and then followed by star chains.

In summary, we have clearly demonstrated that under an elongational flow (1) polymer chains with different topologies are able to ‘‘crawl’’ through a much smaller pore only when the flow rate (q) is higher than their corresponding critical values (q_c), independent of their sizes, and (2) one can effectively and cleanly separate and fractionate star and linear polymer chains in terms of different chain topologies, not their sizes, when the flow rate is properly chosen; namely, $q_{c,\text{star}} > q > q_{c,\text{linear}}$. Further, such a novel method can be developed to separate and fractionate a

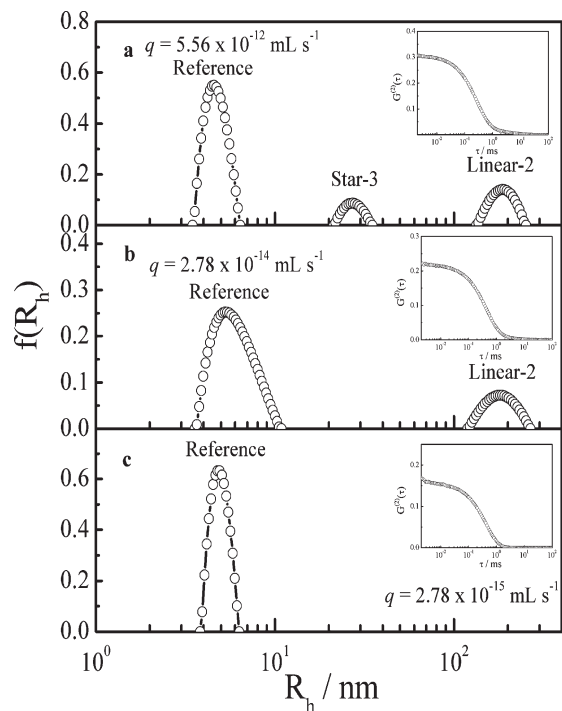


Figure 3. Hydrodynamic radius distribution of a mixture of reference, linear-2, and star-3 chains in toluene at $T = 25\text{ }^{\circ}\text{C}$ after the solution is extruded through nanopores under different elongational flow rates, where $C_{\text{reference}} = 1.80 \times 10^{-2}\text{ g/mL}$, $C_{\text{linear-3}} = 8.00 \times 10^{-6}\text{ g/mL}$, and $C_{\text{star-3}} = 2.50 \times 10^{-4}\text{ g/mL}$. Insets are corresponding time autocorrelation functions.

mixture of polymer chains with different topologies, especially a mixture of linear chains with other topological chains, such as ring and branched chains as long as we know their corresponding critical flow rates. For a mixture of branched chains with different

sizes or star chains with different numbers of arms, we expect that one can separate and fractionate them by gradually increase the flow rate in a step-by-step fashion.

Acknowledgment. The financial support of the National Natural Scientific Foundation of China Project (20934005, B040608) and the Hong Kong Special Administration Region Earmarked Projects (CUHK4037/07P, 2160331; CUHK4046/08P, 2160365; CUHK4039/08P, 2160361; and CUHK4042/09P, 2160396) is gratefully acknowledged.

References and Notes

- (1) Hadjichristidis, N.; Pitsikalis, M.; Pispas, S.; Iatrou, H. *Chem. Rev.* **2001**, *101*, 3747.
- (2) Meunier, D. M.; Smith, P. B. *Macromolecules* **2005**, *38*, 5313.
- (3) Meunier, D. M.; Stokich, T. M., Jr.; Gillespie, D.; Smith, P. B. *Macromol. Symp.* **2007**, *257*, 56.
- (4) Edam, R.; Meunier, D. M.; Mes, E. P. C.; Van Damme, F. A.; Schoenmakers, P. J. *J. Chromatogr., A* **2008**, *1201*, 208.
- (5) De Gennes, P. G. *J. Chem. Phys.* **1974**, *60*, 5030.
- (6) Pincus, P. *Macromolecules* **1976**, *9*, 386.
- (7) Ge, H.; Jin, F.; Li, J. F.; Wu, C. *Macromolecules* **2009**, *42*, 4400.
- (8) Teraoka, I., Ed.; *Polymer Solutions: An Introduction to Physical Properties*; John Wiley & Sons: New York, 2002.
- (9) Perkins, T. T.; Smith, D. E.; Chu, S. *Science* **1997**, *276*, 2016.
- (10) Brochard-Wyart, F.; De Gennes, P. G. *C. R. Acad. Sci., Ser. II* **1996**, *323*, 473.
- (11) De Gennes, P. G. *Adv. Polym. Sci.* **1999**, *138*, 91.
- (12) Lee, H. J.; Lee, K.; Choi, N. *J. Polym. Sci., Part A: Polym. Chem.* **2005**, *43*, 870.
- (13) Hadjichristidis, N.; Iatrou, H.; Pispas, S.; Pitsikalis, M. *J. Polym. Sci., Part A: Polym. Chem.* **2000**, *38*, 3211.
- (14) Zhou, S. Q.; Fan, S. Y.; Au-yeung, S. T. F.; Wu, C. *Polymer* **1995**, *36*, 1341.
- (15) Chu, B. *Laser Light Scattering*, 2nd ed.; Academic Press: New York, 1991.
- (16) Berne, B. J.; Pecora, R. *Dynamic Light Scattering*; Plenum Press: New York, 1976.
- (17) Wang, X. H.; Goh, S. H.; Lu, Z. H.; Wu, C. *Macromolecules* **1999**, *32*, 2786.
- (18) Jin, F.; Wu, C. *Phys. Rev. Lett.* **2006**, *96*, 237801.